SCANNING VOL. 22, 263–270 (2000)
© FAMS, Inc.
Received: November 22, 1999
Accepted: March 17, 2000

Ultrastructure and Reproduction Behaviour of Single CHO-K1 Cells Exposed to Near Infrared Femtosecond Laser Pulses

H. OEHRING, I. RIEMANN, P. FISCHER, K.-J. HALBHUBER, K. KÖNIG

Institute for Anatomy II, Friedrich Schiller University, Jena, Germany

Summary: In the present work, the authors investigated ultrastructural changes as well as the reproduction behaviour of preselected single CHO-K1 cells exposed to 170 femtosecond laser pulses at different power output levels in comparison with cells outside the illumination volume. The ultrashort laser pulses were provided by an 80 MHz Ti:sapphire laser at 780 nm. The cells were scanned ten times with a scan rate of 1/16 s^{-1}. Single CHO-K1 cells exposed to low mean power of 2 mW revealed no significant changes in ultrastructure after laser exposure. In some cases, changes of mitochondria with slight disordering of cristae were found. Cytoplasm was filled with vesicles that seemed to be released from Golgi stacks. Cells irradiated with higher powers demonstrated more dramatic changes in ultrastructure. A considerable number of swollen mitochondria in conjunction with loss of cristae was observed. The main event of mitochondrial changes was the formation of electron dense bodies in the mitochondrial matrix. In addition, lumen of endoplasmatic reticulum was enlarged. Highest applied mean laser power of 12.5 mW lead to complete destruction of mitochondria and their transformation to electron dense structures containing membrane material. Compared with cell targets irradiated with 2 mW mean power, the release of vesicles from Golgi stacks seemed to be rather moderate. Cells localised outside the laser beam revealed no ultrastructural changes. Low mean laser power at 2 mW was unable to impair the reproduction behaviour of CHO-K1 cells. At higher laser power output levels, CHO-K1 cells started to delay cell division. At 12.5 mW, no cell division occurred. The obtained results may be helpful in recommending parameters for safe femtosecond laser microscopy of living specimens.

This work was supported by grants from the German Science Foundation (DFG) DFG (KO 1361/10-1) and from the Ministry for Science, Research and Culture of the Free State of Thuringia (TMWFK).

Address for reprints:

Dr. Hartmut Oehring
Institute for Anatomy II
Friedrich Schiller University
Teichgraben 7
D-07743 Jena, Germany
E-mail: HOehr87712@aol.com

Key words: laser, near-infrared, two-photon microscopy, electron microscopy, reproduction behaviour

PACS: 87.17.-d 87.50-9

Introduction

Near infrared (NIR) laser microscopy has several advantages compared with conventional one-photon laser confocal microscopy. There are no efficient cellular absorbers in the spectral range of 700 to 1200 nm, and subsequently no efficient destructive photothermal nor photochemical processes. The penetration depth of this NIR light is high and on the order of some millimetres in biological tissues. Two-photon and three-photon excitations occur only in a tiny focal volume (< 1 μm^3) of the high-numerical aperture objective. Therefore, out-of-focus photodamage and photobleaching can be avoided; however, photostress may occur in the focal plane. Simultaneous absorption of two photons requires approximately half of the photon energy necessary for one photon excitation. However, light intensities in the range of MW/cm^2 and GW/cm^2 are required compared with W/cm^2 and kW/cm^2 intensities in one-photon microscopy (Denk *et al*. 1990; König *et al*. 1996c, 1997). The high intensities in multiphoton microscopy are realised by the application of ultrashort pulses with high peak and low mean power in the range of some hundred μW up to some mW (König *et al.* 1996c).

Photodamage may result either by cytotoxic reactions (for example, photodynamic reactions) of the exogenous dye added to cell and tissue components or by intracellular endogenous photosensitive absorbers. At very high light intensities, destructive optical breakdown may also occur. Thermal effects play no significant role in NIR microscopy (Liu *et al*. 1995). Endogenous two-photon or three-photon absorbers with photosensitising properties are the reduced coenzymes NADH, NADPH, flavins, porphyrins, and cytochromes (König *et al.* 1995, 1999). Light excitation may result in the formation of oxygen radicals and singlet oxygen. Cell damages can be therefore provoked by photo-induced oxidative stress (König *et al.* 1996 a,b; 1999).

Previous investigations with conventional one-photon He-Ne laser systems and ultraviolet (UV) light sources

demonstrated distinct ultrastructural changes of cell organelles, for example, mitochondria of irradiated target cells (König *et al.* 1999, Manteifel *et al.* 1997, Passarella *et al.* 1988).

The aim of experiments reported in the present paper was to investigate ultrastructural changes of the cell interior by electron microscopy and reproduction behaviour of single CHO-K1 cells exposed to NIR femtosecond laser pulses at different powers. This paper recommends parameters for safe microscopy of living specimen and illustrates interactions between femtosecond laser pulses using a wavelength of 780 nm for irradiation and biological objects. Subsequently, ultrastructure and cell growth values of irradiated target cells were compared with neighbour cells outside the excitation volume.

Material and Methods

Cells

Chinese hamster ovary cells (CHO-K1 ATCC no. 61) were cultivated in monolayers at 37°C and 5% CO_2 in GIBCO's nutrient mixture (HAM F12) supplied with 10% fetal bovine serum and L-glutamine. For laser exposure and the following observation of reproduction behaviour, cells were grown in sterile 2 ml chambers with two round 0.17 mm coverslips as chamber windows (JenLab GmbH, Jena, Germany). Single adherent cell pairs (cells that underwent one cell division) were exposed to the laser beam, marked with a diamond on the outside of the chamber window, and maintained in the incubator for 48 h. With a cell density of about 20.000 ml^{-1}, the typical distance between cell pairs was 150 µm. Viability of cells after laser exposure was tested with a live/dead fluorescence kit consisting of the green fluorescent live cell stain calcein (2 µM) and the red fluorescent dead cell indicator ethidium homodimer (Eth D1, 4 µM, Molecular Probes, Eugene, Ore., USA). The cells were incubated with this viability kit after laser irradiation for 15 min. Fluorescence was induced with two-photon excitation using the NIR laser beam.

For laser exposure with subsequent electron microscopic analysis, cells were cultivated as monolayers in sterile plastic Petri dishes with 3.5 cm diameter. For exposure to the laser beam, cell monolayers in cultivation medium were covered with sterile 0.17 mm coverslips. Single cells preselected for irradiation were marked with a diamond on the outside of the plastic dish. The cell density was the same as described above.

Laser Irradiation

The 780 nm beam of tunable mode-locked 76 MHz titanium-sapphire laser (Mira Model 900-F, Coherent, Santa Clara, Calif., USA), pumped by a 7 W multi-line Ar^+ laser (Innova 310, Coherent) was expanded by an 1:3 Galileian telescope. The equipment was coupled to a modified inverted confocal laser scanning microscope (LSM 410, Zeiss, Jena, Germany). The galvanometer scanning mirrors of the microscope were used to deflect the laser beam in x- and y-direction and to realise beam scanning. A frame rate of 0.0625 s^{-1} (16 s/ frame) was chosen. A high numerical aperture objective (Zeiss Neofluar 40× / numerical aperture 1.30, oil) was used to focus the beam to an aperture-diffraction limited submicron spot.

The pulse duration was measured with an autocorrelator (APE Angewandte Physik Elektronik GmbH, Berlin, Germany) before the beam entered the microscope as well as in the back focal plane of the objective. The mean laser power was measured in the air after transmission through the objective with the power meter Fieldmaster FM (Coherent). Single preselected cells were microirradiated with NIR beam of 170 fs pulse width, 80 MHz repetition frequency, pixel dwell time approximately 80 µs per scan (512×512 pixels covering a sample area of 35×35 µm by the scanning beam), and a total number of 10 scans per cell. The mean power was varied as follows: 2 mW, 3 mW, 7 mW, and 12.5 mW.

Electron Microscopy

One hour after laser irradiation, monolayers of CHO-K1 cells grown on plastic well dishes were fixed for 20 min at 20°C in 2% glutardialdehyde (Fluka, Buchs AG, Buchs, Switzerland) containing 0.1 M cacodylate buffer (pH 7.2, 7% sucrose). After fixation cell monolayers were washed three times with 0.1 M cacodylate buffer (pH 7.2, 7% sucrose) and postfixed with a freshly prepared solution of 1.5% potassium ferrocyanide and 1% osmium tetroxide in 0.1 M cacodylate buffer (pH 7.2) at 4°C for 2 h (Maunsbach 1966). After postfixation, cell monolayers were rinsed with 0.1 M cacodylate buffer until the solution remained clear, dehydrated with graded ethanol series, and placed in pure hydroxypropylmethacrylate (Fluka AG). Following an incubation in a mixture of 1:1 hydroxypropylmethacrylate / Epon 812 (Ferak, Berlin, Germany) for 2 h, cells in plastic well dishes were covered with 100% Epon 812 and cured for 48 h in an oven at 65°C.

Irradiated cells previously marked with diamonds on the outer side of plastic dishes were selected for ultrathin sections by a clockwise, sequential trimming of the specimen block to a mesa with a freshly broken glass knife (Hayat 1989). The height of the obtained mesa did not exceed 50 µm. Afterwards, epon block containing irradiated cells was gently separated from plastic dish material with xylene.

Ultrathin sections (70 nm) were cut with 45° diamond knives (Drukker International B.V., Cuijik, The Netherlands) with an Ultracut S (Leica, Vienna, Austria) and picked up on formvar coated copper grids. Sections were stained in 1% uranylacetate (100% methanol with one drop of 37% acetic acid) for 10 min followed by counterstaining in freshly prepared 0.2% lead citrate for 20 s.

Sections were examined with an EM 902A (Zeiss, Oberkochen, Germany) operating at 80 kV.

Evaluation of Laser-Induced Delay of Cell Growth

Cell divisions of monolayers grown in sterile 2 ml chambers and irradiated at 780 nm with laser beams at different power were evaluated after 24 and 48 h following laser exposure.

Cell growth values (CG) were calculated as follows (Schlegel 1985):

$$CG\ (a) = \ln (n_a/n_0) / \ln 2$$

where n_a is the cell number at time period a (0–24 h, 24–48 h, 0–48 h) and $n_0 = 2$ the cell number at time of laser exposure.

Cells localised in the nearest neighbourhood of the scanning laser beam were defined as control cells. Average CG values were determined for a total of 100 control cells.

For statistical analysis of related samples, the Wilcoxon matched-pairs signed-ranks test was used. Differences between independent samples were analysed with the Mann-Whitney U-test. The significance level was taken at 95%. Statistical calculations were made with the Statistical Package for Social Sciences software (SPSS Inc., Chicago, Ill., USA), release 5.0.2.

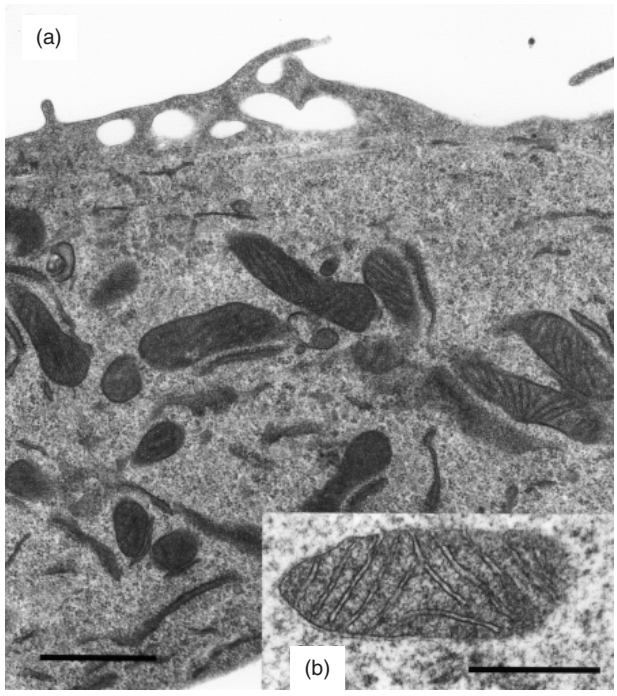

FIG. 1 CHO-K1 cell outside the excitation volume. Distance from scanning laser beam is about 150 µm. (a) Bar 1 µm, (b) bar 0.5 µm.

Results

Transmission Electron Microscopy

CHO-K1 cells outside the excitation volume revealed intact ultrastructure of the nucleus and the cytoplasm (Fig. 1a, b).

Cells irradiated with a mean power output of 2 mW demonstrated only slightly altered mitochondria. Compared with mitochondria of the control cells, local losses of electron-dense material in the mitochondrial matrix could be detected (Fig. 2a, b; asterisks). In some cases, the orientation of cristae is slightly irregular, but the outer mitochondrial membrane is obviously unchanged (Fig 2a, b; arrowheads). In comparison with cells outside the scanning laser beam (Fig. 3) paranuclear regions are filled with an increased amount of vesicles released from Golgi stacks (Fig. 4; arrows). Otherwise the rough endoplasmatic reticulum seems to be unaffected.

Cells irradiated with 3 mW power output clearly demonstrate evident changes in mitochondrial ultrastructure. The mitochondria are remarkably enlarged (Fig. 5a, arrows) combined with a reorientation of cristae (Fig. 5b, arrowheads). Local losses of matrix material could be observed (Fig. 5b, small arrows). In some cases, dense particles could be seen (Fig 5a, arrowheads). Similarly, cytoplasm is filled with numerous Golgi vesicles and vacuoles (Fig. 5a, asterisks).

CHO-K1 cells stressed with a mean power output of 7 mW show formation of enlarged mitochondria with lowered matrix contrast and an irregular distribution pattern of cristae (Fig. 6a, b; asterisks). It is evident that many

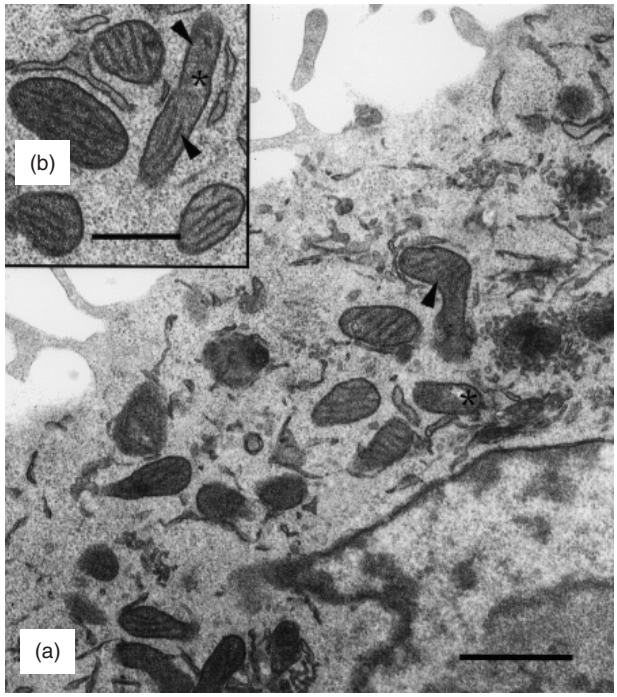

FIG. 2 CHO-K1 cell scanned with a mean power output of 2 mW. Only weak and localised losses of matrix material of mitochondria appeared (*). In a few cases, slight disorderings of cristae could be observed (arrowheads). (a) Bar 1 µm, (b) bar 0.5 µm.

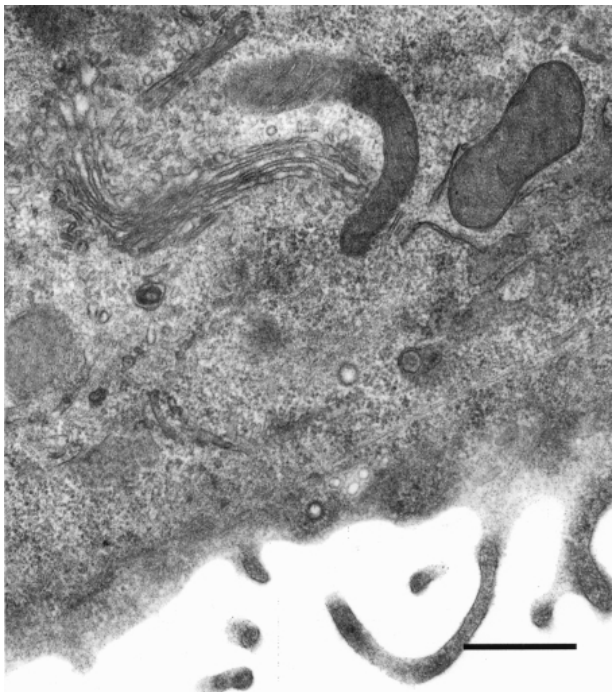

FIG. 3 CHO-K1 cell outside the scanning laser beam. The upper part illustrates Golgi apparatus (G) surrounded by few vesicles. Bar 0.83 μm.

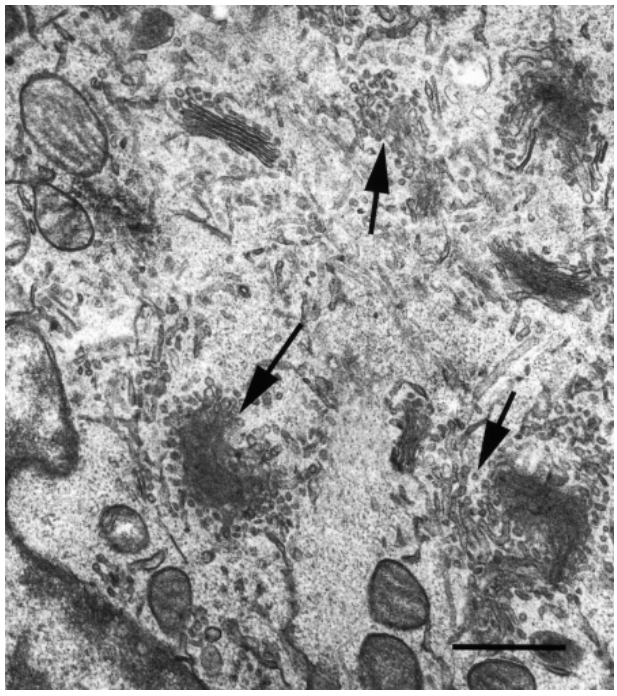

FIG. 4 CHO-K1 cell irradiated with a mean power output of 2 mW. Cytoplasm is filled with vesicles released from Golgi stacks (arrows). Bar 0.83 μm.

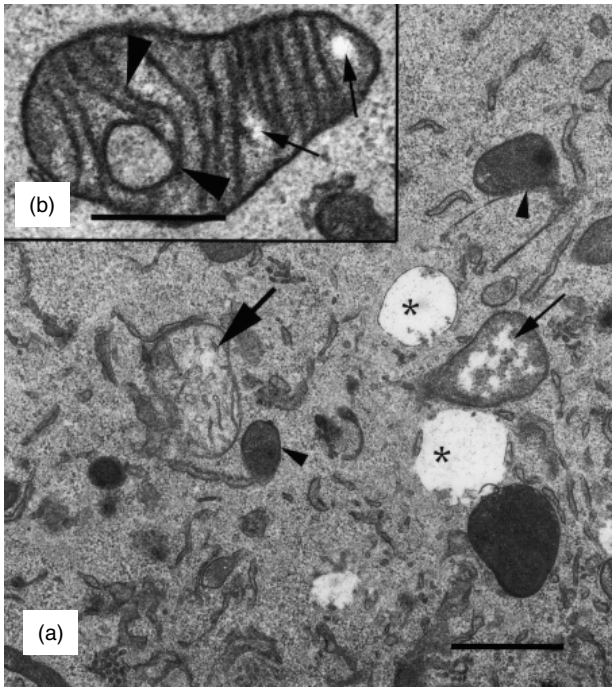

FIG. 5 Target cell irradiated with a mean power output of 3 mW. Cytoplasm contains enlarged mitochondria with disordered cristae (arrows) and distinct loss of matrix material (small arrows). Also, a few dense particles could be detected (arrowheads). In (b) local decreases of matrix contrast (small arrows) and disordered cristae are demonstrated (arrowheads). (a) Bar 1 μm, (b) bar 0.5 μm.

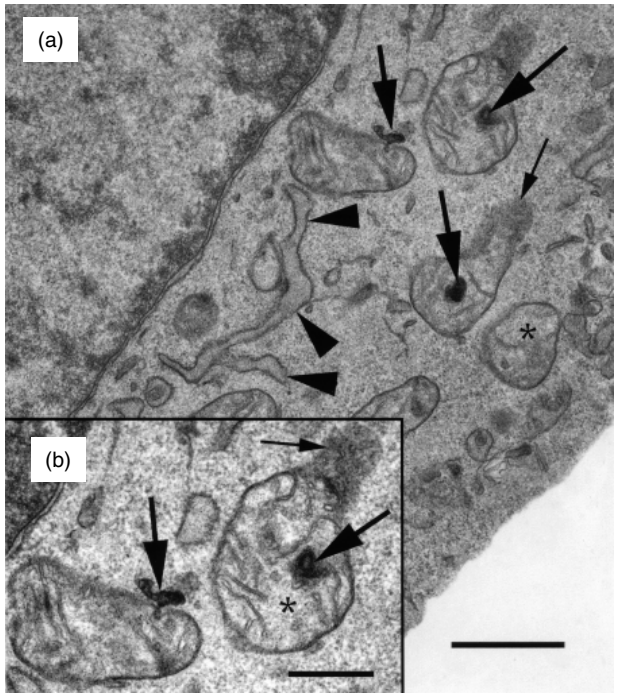

FIG. 6 Cell scanned with a mean power output of 7 mW. Swollen mitochondria are seen in (a) and (b). Arrows show the appearance of osmiophilic bodies inside and outside of enlarged mitochondria. Small arrows indicate diffuse appearance of weak osmiophilic material released from affected mitochondria. The lowered contrast of mitochondrial matrix is shown by (✻). Rough endoplasmatic reticulum appeared to be enlarged (arrowhead). (a) Bar 1 μm, (b) bar 0.5 μm.

mitochondria contain electron dense bodies within the matrix that were observed also outside in the cytoplasm (Fig. 6a, b; arrows). The material obviously released from affected mitochondria is weak osmiophilic (Fig 6a, b; small arrows). The mitochondrial membranes are mostly destroyed and therefore are not clearly visible. The lumen of rough endoplasmatic reticulum is remarkably enlarged and demonstrates low electron contrast (Fig. 6a, arrowheads).

Much more pronounced are the changes at highest applied power output levels in our experimental setup. Figure 7a and b shows a section of a cell irradiated with a mean power output of 12.5 mW that demonstrates numerous electron dense bodies (Fig. 7a, b). Most of investigated mitochondria are heavily affected as indicated by loss of cristae and electron dense matrix material. Such particles (small arrows) often exhibit contacts with lysosomes (asterisks). Electron-dense material can be observed also outside the cytoplasm of irradiated cells (Fig. 7a, arrowheads). Some bodies contain large amounts of membrane material that seems to be derived from completely destroyed mitochondria (Fig. 8b). In Figure 8a and b, a possible transformation of mitochondria into electron-dense bodies is demonstrated (arrowheads).

The cytoplasm of such cells is filled with vesicles obviously derived from Golgi stacks comparable with control cells. The lumen of rough endoplasmatic reticulum appears to be unchanged in comparison with nonirradiated cells.

In contrast to that, no progressive condensation of nuclear chromatin after irradiation at all mean power output levels could be detected. Furthermore, no perturbations of the nuclear envelope were observed.

Cloning Assay of CHO-K1 Cells Irradiated with Near Infrared Femtosecond Laser Pulses

After 48 h, the reproduction behaviour of target cells scanned with a mean power output of 2 mW is significantly enhanced compared with control cells ($p < 0.01$) (Fig. 9). In contrast, the division behaviour of cells exposed to a mean power output of 3 and 7 mW is different from control cells and cell targets scanned with a mean power output of 2 mW. All CG values of cells irradiated with 3 mW are lower by a factor of about 1.36 as CG levels of cells outside the scanning laser beam ($p < 0.05$). Similar but more dramatic delays of cell growth could be observed for target cells irradiated with a mean laser power of 7 mW. In comparison with control cells and target cells exposed to 2 mW power output, CG values are diminished by a factor of about 6.35 ($p < 0.01$). Cell division was completely abolished when cells were irradiated with a mean power output of 12.5 mW.

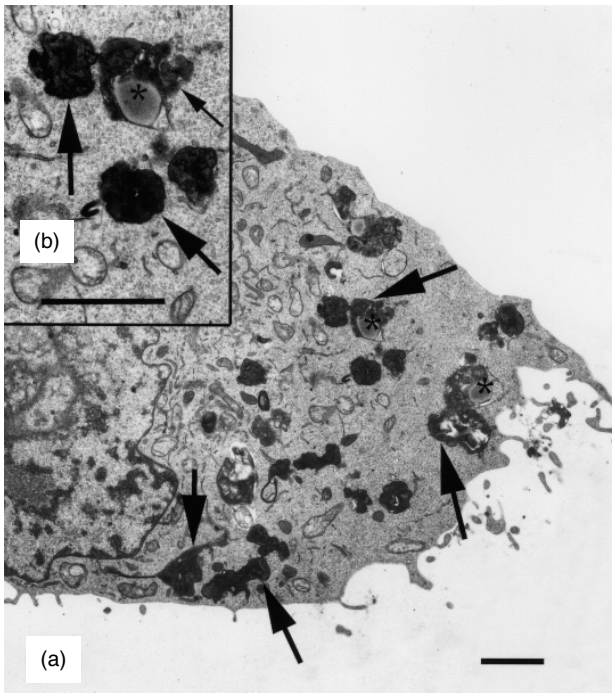

FIG. 7 CHO-K1 cell irradiated with a mean laser power of 12.5 mW. Large osmiophilic bodies are shown in (a) and (b) (arrows). Small arrows in (b) indicate contact between electron dense particles and lysosomes (*). (a) and (b) bar 2 µm.

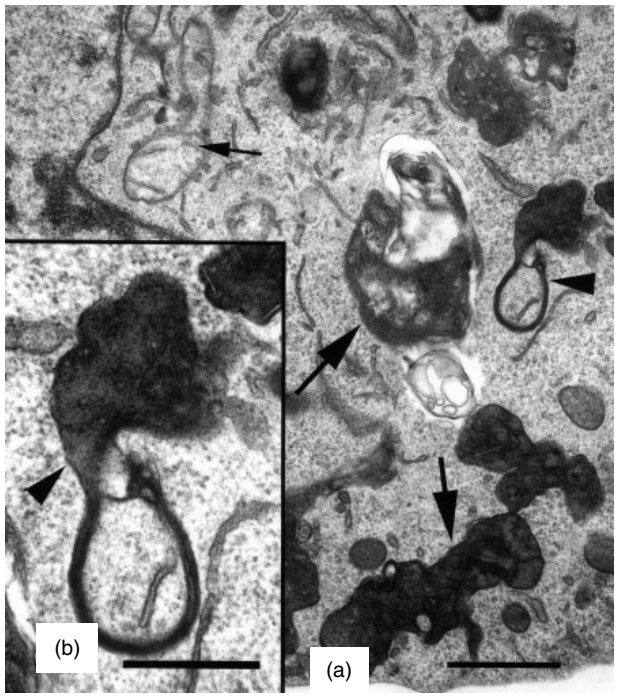

FIG. 8 Target cell scanned with a mean power output of 12.5 mW. Arrowheads in (a) and (b) show transformation of mitochondria to electron dense particles (arrowheads). Furthermore, cytoplasm is filled with osmiophilic particles (arrows). Other mitochondria are deprived from matrix material and cristae (small arrow). (a) Bar 1 µm, (b) bar 0.5 µm.

Discussion

The electron microscopic analysis demonstrates photoinduced effects on ultrastructure. Major targets of NIR femtosecond laser pulses were found to be mitochondria and the Golgi apparatus. Previous investigations undertaken with conventional one-photon laser sources described that protein synthesis of cells as a function of time increased linearly until 60 min (Vacca *et al*. 1996). According to these findings, our experimental setup ultrastructural changes in the time interval 60 min after irradiation were investigated.

First slight effects were found at a mean power of 2 mW. At that power, the reproduction behaviour remained undisturbed; however, cytoplasm of irradiated cells was filled with numerous vesicles released from Golgi stacks. At 3 and 7 mW mean power output, significant changes in ultrastructure correlated with reduced cellular reproduction rate.

König *et al*. (1999) found that damage seems to be based on a two-photon excitation process. Reduced pyridin coenzymes (NADH, NADPH), porphyrins, as well as cytochromes have absorption bands in the UV and are therefore potential targets for near infrared excitation (König *et al.* 1999, Lubart *et al.* 1992). Porphyrins are known to be very potent photosensitizers. Cytochromes, especially cytochrome C oxidase, also have absorption bands at 780 and 830 nm (Lubart *et al.* 1992). They are also capable of generating singlet oxygen as suggested by investigations of Jung and Kim (1990). In low amounts, singlet oxygen is able to accelerate redox activity in the respiratory chain and Ca^{2+} ion influx into cytoplasm stimulating cells mitosis (Friedmann *et al.* 1991). Lipophilic enzymes, such as cytochrome C oxidase of respiratory chain at the inner membrane of mitochondria, are the primary target of singlet oxygen formed by photosensitization (Cernay and Zimmerman 1996). We think that higher power output levels of NIR irradiation lead to enhanced formation of reactive oxygen species, leading to more or less destruction of mitochondrial membranes. Afterwards, endogenous photosensitizers of mitochondria enter the cytoplasm, leading to damage of intracellular membranes (König *et al*. 1996c). Decrease of matrix contrast may indicate loss of matrix components and swelling as well as lowering of enzyme activities, probably accompanied by release of NADP and NADPH into cytoplasm. Release of material derived from affected mitochondria may be indicated by weak osmiophilic material as well as by electron-dense particles in cytoplasm. Formation of electron-dense bodies seems to be the final step of crystal destruction. Previous investigations indicated that such morphologically atypical mitochondria formed after conventional one-photon laser irradiation also contain a disturbed distribution pattern of proteins, DNA, and RNA (Greco *et al.* 1991). Otherwise, the observed condensation of mitochondrial matrix seems to be an alternative process of laser-induced mitochondrial transformations, presumably with concomitant changes of enzyme activities in matrix space. Significantly reduced CG values after irradiation at 7 mW can be related to destructions of cell organelles, especially mitochondria, despite an enlarged lumen of rough endoplasmatic reticulum indicating a stimulated protein synthesis. Highest applied mean power output levels (12.5 mW) led to an appearance of bizarre, electron-dense particles in the cytoplasm of target cells derived from mitochondria, indicating the final step of mitochondrial destruction. Taken together, the main events of all irradiated cells are especially striking, qualitative alterations of cell organelles, first of all of mitochondria with multiple disorderings and losses of cristae as well as of matrix material. In addition, forced release of vesicles from Golgi stacks at 2 mW was remarkable. Hence, mitochondria seem to be the major target for laser light and respond sensitively to photoinduced laser stress even at low power level.

It is known that mitochondria from various tissues have the ability to accumulate Ca^{2+} ions in the matrix compartment by transport processes energetically coupled to the electron transport chain (Lehninger 1970). Experimental results demonstrated that mitochondria of irradiated cells will pull more Ca^{2+} ions into cytoplasm (Breitbart *et al.* 1996, Lubart *et al.* 1997). As has been described by Breitbart *et al.* (1996) and Lubart *et al.* (1997), a precise regu-

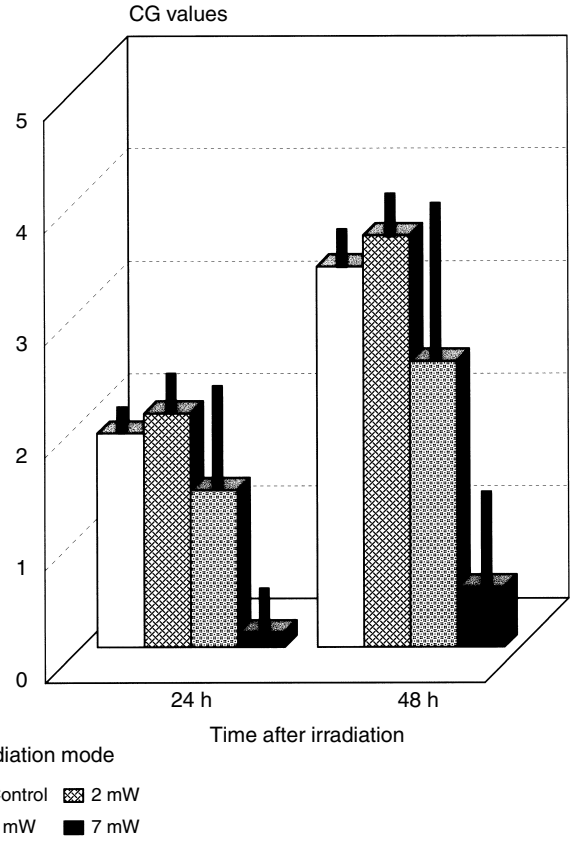

FIG. 9 Cloning assays of irradiated CHO-K1 cells and cells outside the excitation volume. CG values of CHO-K1 cells 24 and 48 h after near infrared irradiation.

lation of the mitochondrial Ca^{2+} and release seems to be important for triggering of mitosis of somatic cells. From this point of view, we presume that forced destructions of mitochondria induced by laser irradiation led to disregulation of intracellular Ca^{2+} levels, also with serious consequences for the cellular reproduction behaviour.

Biochemical experiments undertaken with conventional one-photon laser sources operating with a real power output 7 and 12 mW (Vacca *et al.* 1994, 1996) detected increased synthesis of cytosolic and mitochondrial proteins after irradiation. In addition, increased transcription and translation activities could be found. Moreover, findings described that selective irradiation of mitochondria led to increased electrochemical proton gradients, enhanced adenosine triphosphate (ATP)-synthesis, increased activities of adenosine diphosphate (ADP)-ATP translocator enzyme at the inner mitochondrial membrane (Passarella *et al*. 1994), as well as to activation of mitochondrial matrix enzymes (Greco *et al.* 1991). In addition, recent investigations (Pasarella *et al.* 1994, Yu *et al.* 1997) demonstrated photostimulatory effects on mitochondrial electron transport chain associated with activation of a variety of mitochondrial enzymes. NADPH binding to glutamate dehydrogenase as one key enzyme in the mitochondrial matrix was found to be modified after irradiation with conventional one-photon laser sources (Ostuni *et al.* 1993).

Such photostimulatory processes could explain higher CG values 48 h after scanning with a mean power output of 2 mW. Otherwise irradiation of preselected target cells with higher power output levels (3 and 7 mW) caused pronounced formation of swollen mitochondria with degeneration of cristae. These results are supported by other authors (König *et al.* 1999, Manteifel *et al.* 1997) using conventional one-photon He-Ne and UV light sources. Based on these findings, it can be presumed that such degeneration processes lead to breakdown of the respiratory chain, losses of activities of mitochondrial enzymes, and disregulation of intracellular Ca^{2+} homeostasis, respectively.

In our experimental setup, no morphologically recognisable structures for irradiation-induced apoptosis could be observed. Recent investigations of Kawagishi *et al*. (1998) for effects on ultraviolet B (UVB) irradiation clearly demonstrated that the earliest apoptotic cells appeared at 12 h and reached a peak after 48 h. This is outside our time interval for ultrastructural investigations and should be the topic for long-time studies. Ultraviolet A (UVA) radiation can inhibit mitosis of fibroblasts (Lubart *et al*. 1992). Breaks in DNA strands after UVA exposure could also be demonstrated. It is conceivable that NIR irradiation with highest applied mean power output levels also leads to impaired reproduction behaviour caused by breaks in DNA strands. However, it must be considered that the excitation volume of conventional one-photon microscopy is larger than the detection volume. Photostress and photobleaching are not restricted to the focal plane but occur over the entire depth of the irradiated cell (König *et al*. 1996c). Also, photothermal effects could not be neglected. In contrast, the small subfemtoliter excitation volume of NIR irradiation is limited to the focal plane, allowing high MW/cm^2 intensities, whereas cell regions outside the focal plane are only irradiated with low-intensity NIR radiation (König *et al*. 1996a).

Conclusion

Summarising our experimental results, we conclude that the application of power levels of NIR laser sources for safe microscopy is limited by the preservation of cell organelles. Mitochondria seem to be the most sensitive cellular compartment. Mean power output levels < 2 mW with ≤ 170 fs pulses are recommended for gentle microscopy of living cells. Nonetheless, ultrastructural long-time studies on cells irradiated with pulsed NIR microbeams are necessary.

Acknowledgment

The authors sincerely appreciate the technical assistance of Mrs. Ursula Eschler.

References

Breitbart H, Levinshal T, Cohen N, Friedmann H, Lubart R: Changes in calcium transport in mammalian sperm mitochondria and plasma membrane irradiated at 633 nm (HeNe laser). *J Photochem Photobiol B: Biol* 34, 117–121 (1996)

Cernay T, Zimmermann HW: Selective photosensitization of mitochondria by the lipophilic cationic porphyrin POR 10. *J Photochem Photobiol B*: *Biol* 34, 191–196 (1996)

Denk W, Strickler JH, Webb WW: Two-photon laser scanning microscope. *Science* 248, 73–76 (1990)

Friedmann H, Lubart R, Laulicht I, Rochkind S: A possible explanation of laser-induced stimulation and damage of cell cultures. *J Photochem Photobiol B: Biol* 11, 87–91 (1991)

Greco M, Perlino E, Pastore D, Guida G, Marra E, Quagliariello E: Helium-neon laser irradiation of rat liver mitochondria gives rise to a new subpopulation of mitochondria: Isolation and first biochemical characterization. *J Photochem Photobiol B: Biol* 10, 71–78 (1991)

Hayat MA: *Principles and Techniques of Electron Microscopy. Biological Applications.* Third edition. CRC Press, Inc. Boca Raton, Florida (1989) 164–166

Jung J, Kim HS: The chromophores as endogeneous sensitizers involved in the photogeneration of singlet oxygen in spinach thylakoids. *Photochem Photobiol* 52, 1003–1009 (1990)

Kawagishi N, Hashimoto Y, Takahashi H, Ishida Yamamoto A, Iizuka H: Epidermal cell kinetics of pig skin in vivo following irradiation: Apoptosis induced by UVB is enhanced in hyperproliferative skin condition. *J Dermatol Sci* 18(1), 43–53 (1998)

König K, Liang H, Berns MW, Tromberg BJ: Cell damage by near-IR microbeams. *Nature* 377, 20–21 (1995)

König K, Krasieva T, Bauer E, Fiedler U, Berns MW, Tromberg BJ, Greulich KO: Cell damage by UVA radiation of a mercury microscopy lamp probed by autofluorescence modifications, cloning assay and comet assay. *J Biomed Optics* 1(2), 217–222 (1996a)

König K, Oehring H, Halbhuber KJ, Fiedler U, Bauer E, Greulich KO: Comet assay, cloning assay, light - and electron microscopy on one preselected cell. *SPIE* 3199, 148–155 (1996b)

König K, Simon U, Halbhuber KJ: 3D resolved two-photon fluorescence microscopy of living cells using a modified confocal laser scanning microscope. *Cell Mol Biol* 42(8), 1181–1194 (1996c)

König K, So PTC, Mantulin WW, Gratton E: Cellular response to near-infrared femtosecond laser pulses in two-photon microscopes. *Opt Lett* 22(2), 135–136 (1997)

König K, Becker TW, Fischer P, Riemann I, Halbhuber KJ: Pulse-length dependence of cellular response to intense near-infrared laser pulses in multiphoton microscopes. *Opt Lett* 24(2), 113–115 (1999)

Lehninger AL: Mitochondria and calcium ion transport. *Biochem J* 119, 120–138 (1970)

Liu Y, Cheng DK, Sonek GJ, Berns MW, Chapman CF, Tromberg BJ: Evidence for localized cell heating induced by near infrared optical tweezers. *Biophys J* 68, 2137–2144 (1995)

Lubart R, Wollman Y, Friedmann H, Rochkind S, Laulicht I: Effects of visible and near-infrared lasers on cell cultures. *J Photochem Photobiol B: Biol* 12, 305–310 (1992)

Lubart R, Friedmann H, Sinyakov M, Cohen N, Breitbart H: Changes in calcium transport in mammalian sperm mitochondria and plasma membranes caused by 780 nm irradiation. *Lasers Surg Med* 21, 493–499 (1997)

Manteifel V, Bakeeva L, Karu T: Ultrastructural changes in chondriome of human lymphocytes after irradiation with He-Ne laser: Appearance of giant mitochondria. *J Photochem. Photobiol B: Biol* 38, 25–30 (1997)

Maunsbach AB: The influence of different fixatives and fixation methods on the ultrastructure of rat kidney proximal tubule cells. I. Comparison of different perfusion fixation methods and of GA, FA and osmium tetroxide fixatives. *J Ultrastruct Res* 15, 242–282 (1966)

Ostuni A, Passarella S, Quagliariello E: Photomodulation of glutamate dehydrogenase properties by red light. *J Photochem Photobiol B: Biol* 20, 101–111 (1993)

Passarella S, Roncalli L, Cicero R, Quagliariello E: New ultrastructural conformations of mitochondria irradiated in vitro with a helium–neon laser. *Laser Life Sci* 2(3), 161–171 (1988)

Passarella S, Atlante A, Ostuni A, Pastore D, Quagliariello E: Light–biological system interaction: Mitochondria and isolated enzymes as light targets. *Trends Photochem Photobiol* 3, 307–317 (1994)

Schlegel HG: *Allgemeine Mikrobiologie*. Georg Thieme Verlag Stuttgart, New York (1985) 189–191

Vacca RA, Marra E, Passarella S, Petragallo VA, Greco M: Increase in cytosolic and mitochondrial protein synthesis in rat hepatocytes irradiated in vitro by He-Ne laser. *J Photochem Photobiol B: Biol* 34, 197–202 (1996)

Vacca RA, Marra E, Quagliariello E, Greco M: Increase of both transcription and translation activities following separate irradiation of the in vitro system components with He-Ne laser. *Biochem Biophys Res Comm* 203(2), 991–997 (1994)

Yu W, Naim JO, McGowan M, Ippolito K, Lanzafame RJ: Photomodulation of oxidative metabolism and electron chain enzymes in rat liver mitochondria. *Photochem Photobiol* 66(6), 866–871 (1997)